ELSEVIER

Catalysis Today 78 (2003) 247–256

CATALYSIS TODAY

www.elsevier.com/locate/cattod

# High performance of V–Ga–O catalysts for oxidehydrogenation of propane

A. Pérez Pujol [a], R.X. Valenzuela [a], A. Fuerte [a], E. Wloch [b], A. Kubacka [b], Z. Olejniczak [c], B. Sulikowski [b], V. Cortés Corberán [a,*]

[a] *Institute of Catalysis and Petroleumchemistry, CSIC, Campus Cantoblanco, 28049 Madrid, Spain*
[b] *Institute of Catalysis and Surface Chemistry, Polish Academy of Sciences, Niezapominajek 8, 30-239 Kraków, Poland*
[c] *Institute of Nuclear Physics, Radzikowskiego 152, 31-342 Kraków, Poland*

**Abstract**

The catalytic performance in the oxidehydrogenation (ODH) of propane of vanadium oxide catalysts supported on gallium oxide, $VO_x/Ga_2O_3$, with vanadium coverages lower or near the theoretical monolayer has been studied as a function of the vanadium content and compared with those of other known effective V–M–O (M = Mg, Ca) catalysts. Catalyst activity was very high and increased with the increase of vanadium loading in the range studied, while the selectivity trend was similar for the studied catalysts, excepting that with the lower V content. FT-Raman and $^{51}V$ solid state NMR spectroscopies show that for coverages below the theoretical monolayer vanadium atoms are in tetrahedral co-ordination either in isolated or polymeric species, while the onset of vanadia formation is detected above that coverage. Interestingly, these catalysts show an one order of magnitude higher area-specific rate, similar initial olefin selectivity and slightly higher selectivity decrease with the increase of conversion than the best VMgO catalyst. This is due to the high intrinsic activity of isolated tetrahedral vanadium species. The combination of these factors produces an enhanced olefin productivity of V–Ga–O catalysts.


*Keywords:* Oxidehydrogenation; Oxide catalysts; Propane; Propene; Gallium oxide; Vanadium oxide; Intrinsic activity; Catalytic productivity; NMR; Raman spectroscopy

## 1. Introduction

The practical application of the oxidative route for the dehydrogenation of light alkanes remains still an unresolved scientific and technological challenge in spite of the broad research effort devoted to this goal. The main issue is how to obtain olefin selectivity and productivity that would make this type of process economically feasible. This is due to the over-oxidation of the olefin formed, which in turn decreases the selectivity very sharply with the increase of conversion, thus giving low yields. High selectivity can be attained at low conversion, but the implementation of a process operated at this regime faces the constraint of the low yield per pass and the low catalyst productivity. Thus, besides the selectivity, the catalyst productivity (i.e., its intrinsic activity) needs to be improved further.

Among the large number of catalytic systems for the oxidehydrogenation (ODH) of light alkanes studied, catalysts based on the supported vanadium oxide and its combinations with other oxides are the most efficient [1,2]. The physico-chemical properties of vanadium oxide, and hence its catalytic performance, can be significantly modified by depositing it onto an oxide support. Performance of such catalysts is highly

* Corresponding author. Fax: +34-1-5854760.
*E-mail address:* vcortes@icp.csic.es (V. Cortés Corberán).

0920-5861/02/$ – see front matter © 2002 Elsevier Science B.V. All rights reserved.
PII: S0920-5861(02)00348-6

dependent on the loading of the active oxide, the nature of the support and the interaction between both, while the method of preparation is not affecting significantly its structure [3]. The most remarkable features are observed in such catalysts at low vanadium loadings, i.e., when the surface coverage by vanadia is below the one monolayer [4–6].

Recently, we have reported for the first time that vanadium oxide supported on gallium oxide ($VO_x/Ga_2O_3$) had brought about novel catalysts exhibiting enhanced olefin selectivity for the ODH of ethane and propane [7]. The objective of the present work is to study the performance of V–Ga–O catalysts in the ODH of propane as a function of the vanadium content, at low surface coverage, and to compare them with other known efficient V–M–O catalysts (such as M = Mg, Ca).

## 2. Experimental

*Samples preparation*. Vanadium(V) oxide (p.a.) was dissolved in the solution of oxalic acid. Then the calculated amount of the vanadium oxalate solution was carefully mixed with gallium(III) oxide (Aldrich, surface area $BET_{Ar} = 22.9\,m^2/g$), containing predominantly β-$Ga_2O_3$, about 5% of α-$Ga_2O_3$ and hydroxy gallium oxide (see below). After drying at ambient temperature the samples were calcined in the argon flow at 500 °C for 2 h (heating rate from ambient temperature to 500 °C was 15°/min). The samples were then cooled down, crushed and sieved to give 0.30–0.42 mm fraction used for catalytic tests. Characteristics of the samples, denoted hereinafter as *x*VGa, where *x* is the vanadium superficial coverage of the support, calculated assuming the theoretical monolayer is equal to 9.96 V/nm$^2$ [8], are given in Table 1. To check the influence of the gallium oxide phase, a sample, denoted as 0.5VGa(*B*), was prepared from a larger area support ($BET_{Ar} = 27.5\,m^2/g$), which consists of β-$Ga_2O_3$ (about 95%, the other phase was α-$Ga_2O_3$). The preparation of the reference V–M–O (M = Mg, Ca) samples is reported elsewhere [9].

*XRD*. Powder XRD patterns were acquired on a Siemens powder diffractometer using Ni-filtered Cu Kα radiation.

*BET*. Sorption of argon was measured in a volumetric sorption unit of standard design. The samples were outgassed at 350 °C before the measurement.

*Raman spectroscopy*. Laser Raman spectra were collected at ambient temperature with a resolution of 4 cm$^{-1}$ with a FT Bruker RFS 100 spectrometer, equipped with a liquid-nitrogen-cooled germanium detector. A Nd:YAG laser was used as the excitation source ($\lambda = 1046$ nm), and the beam power on the sample was adjusted as necessary (50–200 mW). For some samples with low vanadium content and therefore exhibiting very weak Raman signal, typically 2048 scans had to be accumulated.

*NMR spectroscopy*. $^{51}V$ solid state static and MAS NMR spectra were acquired on a home-made pulse spectrometer at 78.75 MHz (magnetic field = 7.05 T). A Bruker HP-WB high-speed MAS probe equipped with the 4 mm zirconia rotor and KEL-F cap was used to record the MAS spectra at the spinning speed ranging from 7 to 8 kHz. The free induction decay was recorded after a single 2 μs rf pulse, which corresponded to a $\pi/8$ flip angle for the liquid sample. The repetition rate was 1 s, the spectrum width 250 kHz, and 4 k complex points were acquired. The number of acquisitions ranged from 200 for the $V_2O_5$ sample up to 4000 for the low vanadium-containing samples.

*Catalytic tests*. Catalytic activity for ODH of propane was measured at temperatures between 400 and 550 °C under atmospheric pressure. Catalyst particles (0.1 g, 0.42–0.59 mm) were loaded into a tubular,

Table 1
Characteristics of calcined samples prepared by deposition of vanadium oxalate on gallium(III) oxide

| Sample | Support $BET_{Ar}$ ($m^2/g$) | $V_2O_5$ (wt.%) | V (atom/nm$^2$) | $\theta$[a] | Sample $BET_{Ar}$ ($m^2/g$) |
|---|---|---|---|---|---|
| 0.2VGa | 22.9 | 0.65 | 1.9 | 0.19 | 22.5 |
| 0.5VGa(*B*) | 27.5 | 1.96 | 4.8 | 0.48 | 15.9 |
| 0.5VGa | 22.9 | 1.79 | 5.3 | 0.53 | 20.6 |
| 1.1VGa | 22.9 | 3.52 | 10.6 | 1.06 | 20.2 |

[a] Vanadium superficial coverage of the support, calculated assuming the theoretical monolayer is equal to 9.96 V/nm$^2$ [8].

down-flow quartz reactor. SiC chips were placed above the catalyst to reduce the undesired free volume. A propane–oxygen mixture (in molar ratios 0.5, 1 and 2) diluted in helium was fed into the reactor at a total flow of 100 ml/min and contact time of 12.3 g h/mol $C_3$, unless stated otherwise. Reactants and products were analysed on-line by gas chromatography using two packed columns filled with molecular sieve (for $O_2$ and CO) and Porapak Q (for the rest). In all experiments the mass and carbon balances were within 100 ± 5%.

## 3. Results and discussion

### 3.1. Bulk characterisation

The chemical analysis showed that the vanadium contents of the final samples agree well with the theoretical value (Table 1). The incorporation of vanadium onto the support did not modify the XRD patterns of the supports as shown in Fig. 1. The pattern of sample 0.5VGa(*B*) is equivalent to that of its support that corresponds to that of β-$Ga_2O_3$. For the rest of the samples, prepared with the low surface area $Ga_2O_3$, the XRD pattern was much less intense with poorer signal-to-noise ratio. The peaks could be assigned to those of the β-$Ga_2O_3$, although those corresponding to α-$Ga_2O_3$ and hydroxy gallium oxide were also present, however, with a much lower intensity. We may conclude that no new phase was formed by the interaction between the both oxides.

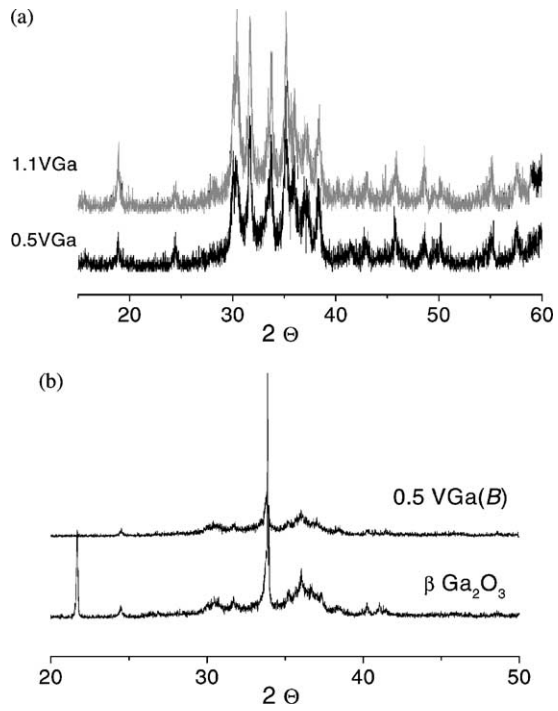


Fig. 1. XRD patterns of the $VO_x/Ga_2O_3$ catalysts prepared with (a) lower surface area and (b) higher surface area gallium oxide supports.

### 3.2. Surface characterisation

As shown in Table 1, deposition of a small amount of vanadium oxide did not modify the BET specific surface area of the support for the 0.2VGa sample. Deposition of a higher amount decreased it for samples 0.5VGa and 1.1VGa. The decrease of BET area was even more pronounced for the sample with the larger area support (0.5VGa(*B*)), what seems to point to a possible blocking of pores by the vanadium oxide in this case.

The nature of the surface vanadium species was initially investigated by FT-Raman spectroscopy, and their spectra are shown in Fig. 2. The Raman spectrum of pure β-$Ga_2O_3$ shows lines at 112, 144, 168, 199, 320, 345, 416, 475, 629, 653 and 765 $cm^{-1}$ (Fig. 2). The bands in the range 300–600 $cm^{-1}$ correspond to bending vibrations, while the signal at 770 $cm^{-1}$ is due to the Ga–$O_4$ tetrahedral stretching mode [10]. For the VGa samples a very weak Raman signal and a high fluorescence were observed. Consequently, only spectra with low signal-to-noise ratio could be obtained, despite the conditions of the measurement. The spectrum of the lowest vanadium content sample, 0.2VGa, was practically identical to that of the support, probably due to the very low amount of deposited vanadium. However, upon subtracting the spectrum of the support, a weak broad band around 660–800 $cm^{-1}$ and a very weak band around 1000 $cm^{-1}$ could be detected in the difference spectrum (not shown). In the other VGa samples, the signals were very broad and the fluorescence more intense. The lines corresponding to $Ga_2O_3$ were either completely suppressed or very weak, even the most intense line at 199 $cm^{-1}$. Besides these lines, the spectrum of the 0.5VGa sample showed only one intense broad band around 600–780 $cm^{-1}$, with maximum at 760 $cm^{-1}$, and a weaker one with

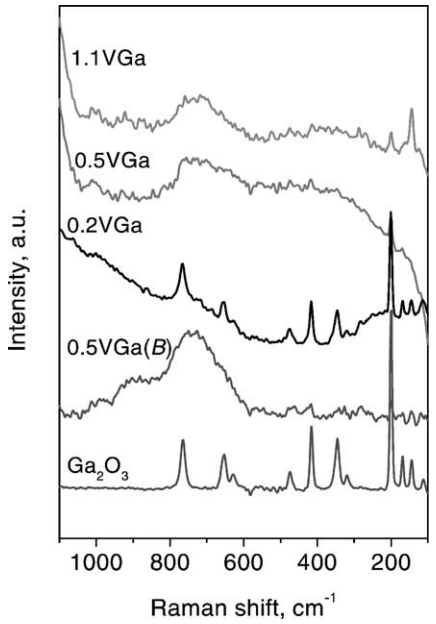


Fig. 2. Raman spectra of $VO_x/Ga_2O_3$ catalysts: (a) β-$Ga_2O_3$; (b) 0.5 VGa(*B*); (c) 0.2VGa; (d) 0.5VGa; (e) 1.1VGa. The spectra of all the mixed oxide samples have been baseline corrected and their intensity enhanced by a factor of 3.

maximum at 1010 $cm^{-1}$, a pattern similar to the difference spectrum of 0.2VGa. Upon increasing vanadium content, some other features are also seen in the spectrum of 1.1VGa, similar to those observed for VGa samples with a higher vanadium content [7]. These are a sharp band at 145 $cm^{-1}$ and other weaker ones at 284, 525, 715 (shoulder) and 993 $cm^{-1}$, assigned to crystalline $V_2O_5$ [11], which may indicate the onset of the formation of this phase on the surface, and two broad bands at 880 and 920 $cm^{-1}$, that may be assigned to polyvanadates with tetrahedral coordination as in magnesium pyrovanadates [12,13]. These two broad bands seem to be merged in the spectrum of the 0.5VGa(*B*) sample, which also shows the more intense broad band around 600–780 $cm^{-1}$ observed for sample 0.5VGa, with its maximum slightly shifted to lower Raman shift values, and the broad band around 1010 $cm^{-1}$. As the spectra were collected under ambient conditions, this latter band, present in all the spectra of V–Ga–O samples, can be attributed to the characteristic stretching symmetric vibration of terminal V=O groups in isolated $VO_4$ tetrahedra ($O_3$–V=O mono oxo species), which appears at 1020–1034 $cm^{-1}$ in dehydrated $VO_x/\gamma$-$Al_2O_3$, shifting to lower Raman shift values under ambient conditions [14]. The assignment of the more intense band at 765 $cm^{-1}$ is not so straightforward. The profile of this band resembles the single broad band observed previously in the Raman spectra of a 24 wt.% $V_2O_5$/CaO [9] and a 6.67 wt.% vanadia supported on sepiolite [15] catalysts, that were assigned to highly distorted, isolated tetrahedral vanadium species, but in these cases the maximum was at 809 $cm^{-1}$ with a shoulder at 785 $cm^{-1}$. On the other hand, the bands characteristic for V–O–V stretching modes appear at 780 $cm^{-1}$ for dimeric tetrahedral vanadate-type species, as in magnesium pyrovanadate [16] and at 745–768 $cm^{-1}$ for octahedral species, as in magnesium metavanadate [16]. However, in such cases these are not the strongest bands of the spectra, which appear at higher Raman shifts.

Hardcastle et al. [17], based on the diatomic approximation, have developed correlations between the Raman stretching frequencies and the bonding length and bond order of the V–O bond, and according to those correlations, the $\nu$(V–O) frequency for the ideal $VO_4$ tetrahedra will be $796 \pm 20$ $cm^{-1}$. Using these correlations one may estimate that for $\nu$(V–O) frequency of 765 $cm^{-1}$, the bond order is 1.17, something lower to the value determined for the orthovanadate $Mg_3V_2O_8$, and the bond length of 0.174 nm, slightly longer than in $Mg_3V_2O_8$, where vanadium atoms are in isolated tetrahedral positions [18]. Consequently, the largest signal around 765 $cm^{-1}$ for sample 0.5VGa may be assigned to the isolated tetrahedral V–O species. A clue to understand the 35 $cm^{-1}$ shift observed, and the broadness of the band, may come from the similarity between vanadium and gallium ions. Both elements share the same Pauling electronegativity (1.6) and the ionic radii of $V^{5+}$ (0.059 nm) and $Ga^{3+}$ (0.062 nm) are very close. Thus, one should expect that the frequency of the stretching modes of the oxygen atoms linking the vanadium atoms in isolated tetrahedra to the gallium atoms of the support, $\nu$(V–O–Ga), must be close to and intermediate between those corresponding to the bridging oxygens in each single oxide, $\nu$(V–O–V) and $\nu$(Ga–O–Ga). This is the case for the main band in the 0.5VGa spectrum. Accordingly, we may suggest that V is present on the 0.5VGa surface as isolated $VO_4$ tetrahedra, highly distorted as shown by the broadness of the band. This assignment is corroborated by

the presence of the band at 1010 $cm^{-1}$. The presence of additional polyvanadate species in the 0.5VGa(*B*) agrees well with the higher specific surface area loss in this sample.

Further evidence on the nature of the vanadium species was obtained by $^{51}V$ NMR spectroscopy. Natural abundance of $^{51}V$ is 99.76%, which makes it possible to follow in detail the local environment of vanadium in solid catalysts. The analysis is, however, complicated by the fact that the $^{51}V$ NMR signal may be complex due to dipolar interactions, quadrupolar interactions and chemical shift anisotropy. Applying high field is favourable in such a case. In contrast to other nuclei extensively used in the structure determination of solids, such as $^{29}Si$, $^{27}Al$, $^{71}Ga$ and $^{11}B$, the NMR lineshape of $^{51}V$ in high magnetic field is dominated by chemical shift anisotropy [19,20]. It should be pointed out clearly that the isotropic chemical shift alone, as determined from the position of the central band in the MAS NMR spectrum, is insufficient to discriminate between different coordinations of vanadium species. It is therefore necessary to measure both the static and MAS NMR spectra. A fundamental information provided by the MAS NMR spectrum is the number of non-equivalent positions of vanadium ions in the solid, as may be determined from the number of central bands. Based on this, a detailed analysis of the static spectrum can be carried out. In favourable cases of only few non-equivalent positions, it is possible to determine the coordination, local symmetry, and the type of association of vanadium polyhedra by comparison with the spectra of model compounds, accompanied by numerical simulation. Since the $^{51}V$ NMR spectra are extremely sensitive to any distortions of local symmetry, the hydration and calcination processes and their influence on the coordination of the vanadium complexes can also be studied.

The static (wide line) and MAS spectra of samples 0.5VGa and 1.1VGa are visualised in Fig. 3a and b, respectively. The central bands in the MAS spectra are marked by an asterisk. The static spectrum of sample 0.5VGa shows an asymmetric and relatively broad pattern. The components of the chemical shift tensor $\delta_1$, $\delta_2$ and $\delta_3$ have been measured from the characteristic points in the static spectrum, and their values are given in Fig. 3a, bottom. The chemical shift anisotropy is large and amounts to about 820 ppm. The isotropic chemical shift was calculated as being $\delta_{iso} = -380$ ppm. This is in rather good agreement with the isotropic chemical shift read out from the MAS spectrum of this sample (Fig. 3b, bottom), measured at 7 kHz spinning speed. Although a central line at ca. −430 ppm and two spinning sidebands represent a single species, as confirmed by measuring the MAS spectrum at various spinning speeds (not shown), the rather large linewidths may be due to certain degree of disorder characterising the vanadium complexes existing in the sample. The NMR results suggest that in this sample vanadium ions occupy the isolated tetrahedral positions. They are characterised by the large chemical shift anisotropy, pointing out to a strong distortion of the vanadium tetrahedra. The interaction of vanadium with the gallium oxide is strong for the sample 0.5VGa ($\theta = 0.53$ theoretical monolayer), and stronger than that observed earlier for the $VO_x/Al_2O_3$ system.

Upon increasing the content of vanadia to about 1.1 theoretical monolayer, the entire spectrum changes its appearance dramatically (Fig. 3b, top). Both the isotropic chemical shift, equal to −616 ppm, and rather large chemical shift anisotropy point out to $V_2O_5$ as a dominating species. This is due to the onset of vanadium pentoxide in this catalyst. The NMR results are in good agreement with the Raman spectra, corroborating the presence of highly distorted tetrahedral species in both samples, and the onset of $V_2O_5$ formation when the vanadium contents is over the theoretical monolayer.

### 3.3. Catalytic properties

Under the reaction conditions used, all the $VO_x/Ga_2O_3$ catalysts were very active for the ODH of propane, showing up to 5% conversion already at 350 °C. The main products were propene, CO and $CO_2$, and their selectivity patterns observed experimentally fitted well to those of a typical parallel–consecutive reaction scheme. No partially oxygenated compounds were observed, and formation of some ethene was detected at the higher temperatures. The apparent activation energies were similar for the 0.5VGa and 1.1VGa samples, 20 ± 2 and 19 ± 2 kcal/mol, respectively, and slightly higher for the 0.2VGa sample (25 ± 2 kcal/mol). As can be seen in Fig. 4, the propane conversion increased with vanadium content, a trend opposite to that of surface areas, which tend to decrease for the higher vanadium

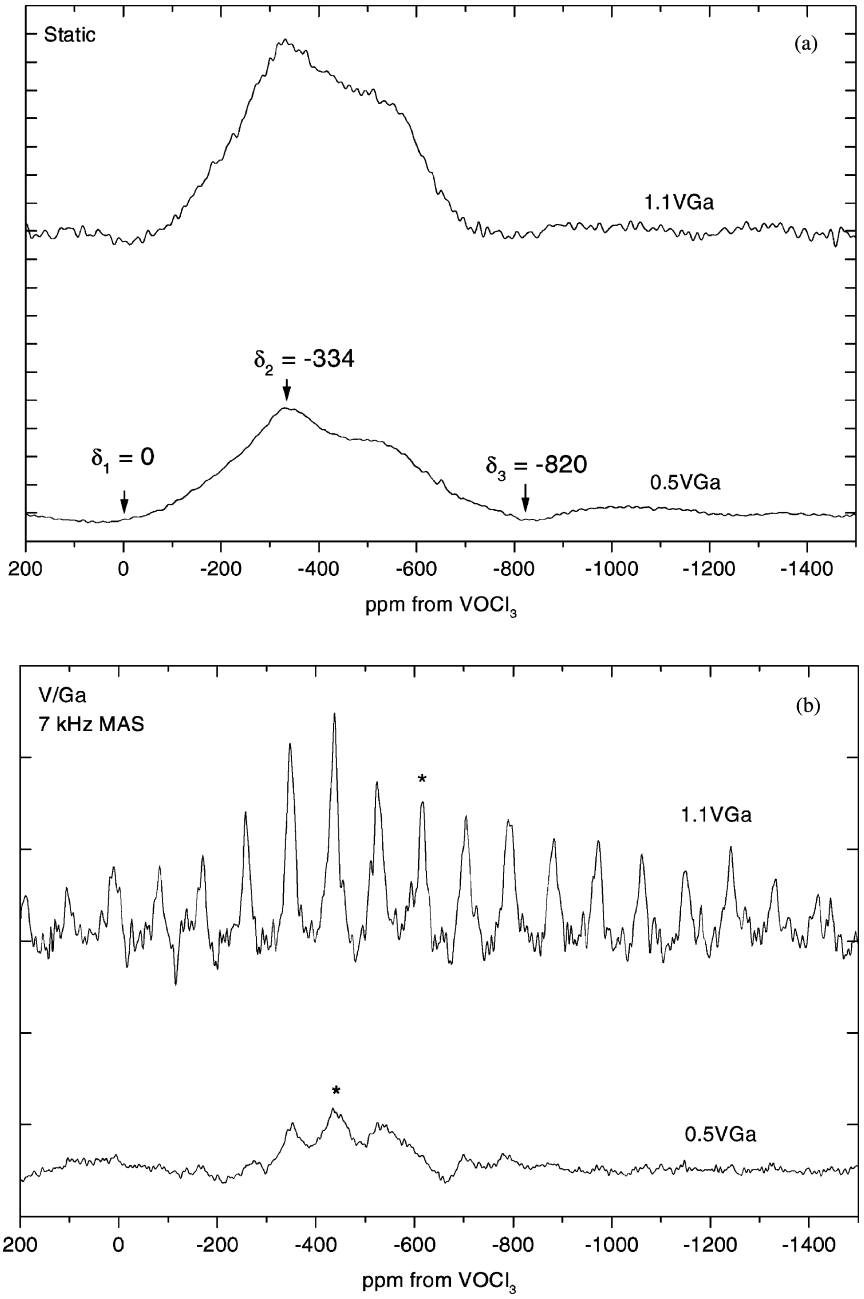


Fig. 3. The 78.75 MHz solid-state $^{51}V$ static (a) and MAS (b) NMR of $VO_x/Ga_2O_3$ catalysts. The central bands of the MAS NMR spectra are indicated by an asterisk.

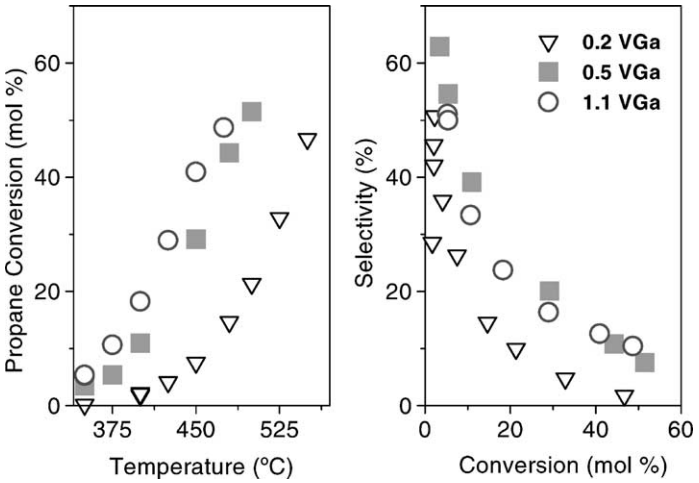


Fig. 4. ODH of propane on VGa samples: conversion of propane vs. reaction temperature (left) and selectivity to propene as a function of propane conversion (right). $C_3H_8$:$O_2$:He = 4:8:88; $W/F = 12\,g_{cat}\,h/mol\,C_3$.

contents (cf. Table 1). It should be noted that the bare $Ga_2O_3$ exhibits some catalytic activity at the reaction conditions used. However, in this case the conversion is more than one order of magnitude lower than that found on any VGa sample, becoming detectable at 425 °C and just reaching 1.5% at 480 °C, and the main products are carbon oxides. As may be seen in Fig. 4, with the exception of the 0.2VGa sample, all the VGa catalysts behaved very similarly, showing an initial olefin selectivity (extrapolated at zero conversion) close to 70%, a value that increases up to 80% when the oxygen-to-propane ratio is decreased to 1. The most active catalyst was 1.1VGa, with area-specific rates almost 70% higher than for the 0.5VGa sample. However, the 0.5VGa catalyst showed consistently higher selectivity to olefin at isoconversion levels of propane, which may be explained by the presence of $V_2O_5$ in the 1.1VGa sample (cf. NMR studies). As could be expected, over every catalyst the selectivity to both $CO_2$ (15–37%) and CO (22–67%), as well as the $CO/CO_2$ ratio (always higher than 1), increased with the increase of conversion. At equal conversion, the higher the V contents, the higher the $CO/CO_2$ ratio. Similar effects have been reported for this reaction over other vanadium-containing catalysts, such as V/sepiolite [15], V–P–O [21], or $V/ALPO_4$ and VAPO-5 [22]. These effects point to a different route of formation of CO and $CO_2$, the former from propene and the latter from both propane and propene, and a faster degradation of propene to CO when the vanadium contents increases.

The performance of the 0.5VGa(*B*) was studied at a lower temperature range by using a higher value of the reciprocal of the space velocity, $W/F = 55\,g_{cat}\,h/mol\,C_3$. Under these conditions, the conversion of propane reached 3.3% (71% olefin selectivity) at 300 °C. The results are compared in Fig. 5 with those of sample 0.5VGa to study the effect of the support. Interestingly, within the experimental error, the results of both catalysts were equivalent at the same reaction temperature, and followed the same trace in the graphs of rate vs. temperature as well as selectivity vs. conversion. This indicates that the catalytic properties of V–Ga–O catalysts are influenced predominantly by the vanadium surface coverage and not by the nature of the gallium oxide support.

### 3.4. Comparison with other V–M–O systems

The high activity showed by these $VO_x/Ga_2O_3$ catalysts guided us towards a direct comparison of their performance with the other V–M–O catalysts. Among these, the V–Mg–O catalysts are known to exhibit high efficiency in the ODH of propane [23,24], and there is a general agreement that the optimal composition corresponds to a 24 wt.% of $V_2O_5$ [1,23,25],

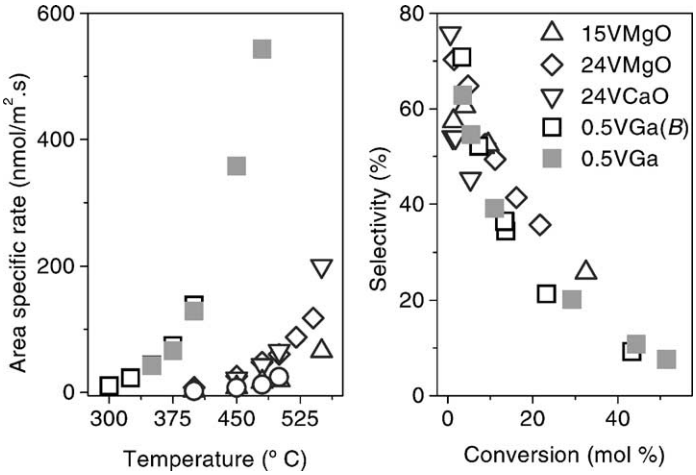


Fig. 5. Comparison of catalytic properties of catalysts 0.5VGa, 0.5VGa(*B*) and V–M–O (M = Mg, Ca) in the ODH of propane: reaction rate vs. reaction temperature (left) and selectivity to propene as a function of propane conversion (right). $C_3H_8$:$O_2$:He = 4:8:88; $W/F = 12\,g_{cat}$ h/mol $C_3$, except for 0.5VGa(*B*), $55\,g_{cat}$ h/mol $C_3$.

usually denoted as 24VMgO. Valenzuela and Cortés Corberán [9] reported recently that a V–Ca–O catalyst with the same vanadium contents (i.e. 24VCaO) showed an area-specific rate equivalent to that of 24VMgO in spite of much lower surface concentration of vanadium. Although 1.1VGa was the most active catalyst, we chose 0.5VGa sample for the comparison, because it shares the same type of vanadium environment on their surface as the catalysts to be compared with, i.e., isolated and/or polymeric tetrahedral vanadium species. As shown in Fig. 5, the V–Ga–O catalysts show a much higher area-specific rate that any of the V–Mg–O or V–Ca–O catalysts. The initial selectivity to olefin is very close for the three catalytic systems. However, the decrease of selectivity with the increase of conversion follows the order V–Mg–O < V–Ga–O < V–Ca–O. As the difference in selectivity at isoconversion levels between V–Mg–O and V–Ga–O is small, the much higher activity of the latter could mean, from a practical point of view, a much higher propene productivity for the V–Ga–O catalysts as compared with the V–Mg–O catalysts.

Finally, another interesting point to be considered is the intrinsic rate of the vanadium centres, as the higher catalytic activity of the 0.5VGa corresponds to the catalysts with the lower vanadium content. Indeed, an exact comparison should be made by calculating the turnover numbers for each type of centre. This, in turn, would require the exact determination of the total number of vanadium atoms at the surface, that could not be determined by the techniques used in this work. However, one can make an estimation based on XPS surface composition. Taking into account the power used in the X-ray source for XPS experiments, the maximum depth of the analysis should not be greater than a very few monolayers. So we may use, in a first approximation, the XPS atomic ratios as representative of the outermost layer, and the XPS V/(V + M) ratio (M = Mg, Ca, Ga) as a relative measurement of the number of vanadium centres on the catalyst surface. In this way, the ratio between area-specific rate and this surface V/(V + M) ratio should be directly proportional to the turnover number of the vanadium surface centres, and we may compare their values as a relative measure of the 'intrinsic' rate of each centre. Table 2 summarises some representative data of the three catalytic systems to facilitate the comparison. At variance of the V–Mg–O and V–Ca–O systems, XPS analysis shows a surface enrichment in vanadium for the 0.5VGa catalyst, which is consistent with the absence of chemical reaction between vanadium oxide and the oxidic support. Even so, the relative activity per surface vanadium atom in the 0.5VGa catalysts is still much higher: over a fortyfold increase compared to 24VMgO and more

Table 2
Comparison of properties of V–M–O catalysts (M = Mg, Ca, Ga)

| | Catalyst | | |
|---|---|---|---|
| | 24VMgO | 24VCaO | 0.5VGa |
| $V_2O_5$ content (wt.%) | 25 | 23.2 | 1.79 |
| BET surface area ($m^2/g$) | 41.5 | 6.0 | 20.6 |
| Ratio V/M (M = Mg, Ca, Ga) | | | |
| Bulk | 0.1389 | 0.1945 | 0.0188 |
| XPS | 0.1067 | 0.0054 | 0.0282 |
| Surface species | Mainly $Mg_3(VO_4)_2$, $Mg_2V_2O_7$, low crystallinity | Isolated $VO_4$ tetrahedra | Isolated $VO_4$ tetrahedra |
| Conversion (mol%) at 480 °C | 8.8 | 1.15 | 44.3 |
| Area-specific rate (nmol/$m^2$ s) at 480°C | 46.6 | 43.4 | 543 |
| Relative activity per surface V atom[a] at 480 °C | 437 | 8040 | 19300 |

[a] Area-specific rate/$(V/(V + M))_{XPS}$ ratio, see explanation in the text.

than twofold in comparison with 24VCaO. This is in good agreement with our previous results [9], demonstrating clearly that the isolated tetrahedral vanadium species are much more active than the polymeric tetrahedral ones.

## 4. Conclusions

Vanadium oxide catalysts supported on gallium oxide, $VO_x/Ga_2O_3$, with vanadium coverage lower than or near the theoretical monolayer, constitute a highly efficient catalytic system for the ODH of propane, with a substantially higher activity than other well-known binary V–M–O catalysts coupled with a good selectivity to olefin. These features stem from the nature of the vanadium surface centres, which are present in the form of isolated tetrahedral species. The combination of their higher activity and slightly reduced selectivity has lead to an enhanced propene productivity over these V–Ga–O catalysts, as compared with the performance of the best V–Mg–O compositions. Additional studies are therefore needed to improve their selectivity characteristics further.

## Acknowledgements

The Polish Academy of Sciences/CSIC Interchange Agreement (Project 2001PL0005) and the Spanish CICYT (Project MAT99-0648) financed this work. The authors thank Dr. Z. Schay for the XPS measurements.

## References

[1] E.A. Mamedov, V. Cortés Corberán, Appl. Catal. A 127 (1995) 1, and references therein.
[2] M.A. Bañares, Catal. Today 51 (1999) 319.
[3] T. Murakami, M. Inomata, K. Mori, T. Ui, K. Suzuki, A. Miyamoto, T. Hattori, Stud. Surf. Sci. Catal. 16 (1983) 531.
[4] S.T. Oyama, G.T. Went, K.B. Lewis, A.T. Bell, G.A. Somorjai, J. Phys. Chem. 93 (1989) 6786.
[5] G. Deo, I.E. Wachs, J. Phys. Chem. 95 (1991) 5889.
[6] N. Das, H. Eckert, H. Hu, I.E. Wachs, J.F. Walzer, F.J. Feher, J. Phys. Chem. 97 (1993) 8240.
[7] B. Sulikowski, A. Kubacka, E. Wloch, Z. Schay, V. Cortés Corberán, R.X. Valenzuela, Stud. Surf. Sci. Catal. B 130 (2000) 1889.
[8] F. Roozeboom, T. Fransen, P. Mars, P.J. Gellings, Z. Anorg. Allg. Chem. 449 (1979) 25.
[9] R.X. Valenzuela, V. Cortés Corberán, Topics in Catal. 11–12 (2000) 153.
[10] D. Dohy, G. Lucazeau, A. Revcolevschi, J. Solid State Chem. 45 (1982) 180.
[11] T.R. Gilson, O.F. Bizri, N. Cheetam, J. Chem. Soc., Dalton Trans. (1973) 291.
[12] W.P. Griffith, T.D. Wickins, J. Chem. Soc. A (1966) 1087.
[13] M.L. Occelli, J.M. Stencel, ACS Symp. Ser. 375 (1988) 195.
[14] S.S. Chan, I.E. Wachs, L.L. Murrell, L. Wang, W. Keith Hall, J. Phys. Chem. 88 (1984) 5831.
[15] A. Corma, J.M. López Nieto, N. Paredes, M. Pérez, Appl. Catal. A 97 (1993) 159.
[16] J. Hanuza, B. Jezowska-Trzebiatowska, W. Oganowski, J. Mol. Catal. 29 (1985) 109.
[17] F.D. Hardcastle, I.E. Wachs, H. Eckert, D.A. Jefferson, J. Solid State Chem. 90 (1991) 194.
[18] N. Krishnamachari, C. Calvo, Can. J. Chem. 49 (1971) 1629.
[19] O.B. Lapina, V.M. Mastikhin, A.A. Shubin, V.N. Krasilnikov, K.I. Zamaraev, Prog. NMR Spectrosc. 24 (1992) 457.

[20] V.M. Mastikhin, O.B. Lapina, in: D.M. Grant, R.K. Harris (Eds.), Encyclopaedia of NMR 8 (1996) 4892.
[21] P.M. Michalakos, M.C. Kung, I. Jahan, H.H. Kung, J. Catal. 140 (1993) 226.
[22] P. Concepción, J.M. López Nieto, J. Pérez Pariente, J. Mol. Catal. A 99 (1995) 173.
[23] M.A. Chaar, D. Patel, M.C. Kung, H.H. Kung, J. Catal. 105 (1987) 403.
[24] H.H. Kung, Adv. Catal. 40 (1994) 1.
[25] T. Blasco, J.M. López Nieto, Appl. Catal. A 157 (1997) 117, and references therein.